Hydrol. Earth Syst. Sci. Discuss., 12, 2527–2559, 2015
www.hydrol-earth-syst-sci-discuss.net/12/2527/2015/
doi:10.5194/hessd-12-2527-2015

Hydrology and Earth System Sciences
Open Access
Discussions

Characterization of precipitation product errors across the US using multiplicative Triple Collocation

S. H. Alemohammad[1], **K. A. McColl**[1], **A. G. Konings**[1], **D. Entekhabi**[1], and **A. Stoffelen**[2]

[1]Department of Civil and Environmental Engineering, Massachusetts Institute of Technology, Cambridge, MA, USA
[2]Koninklijk Nederlands Meteorologisch Instituut (KNMI), R&D Satellite Observations, De Bilt, the Netherlands

Received: 19 January 2015 – Accepted: 13 February 2015 – Published: 27 February 2015

Correspondence to: S. H. Alemohammad (hamed_al@mit.edu)

Published by Copernicus Publications on behalf of the European Geosciences Union.

Abstract

Validation of precipitation estimates from various products is a challenging problem, since the true precipitation is unknown. However, with the increased availability of precipitation estimates from a wide range of instruments (satellite, ground-based radar, and gauge), it is now possible to apply the Triple Collocation (TC) technique to characterize the uncertainties in each of the products. Classical TC takes advantage of three collocated data products of the same variable and estimates the mean squared error of each, without requiring knowledge of the truth. In this study, triplets among NEXRAD-IV, TRMM 3B42, GPCP and GPI products are used to quantify the associated spatial error characteristics across a central part of the continental US. This is the first study of its kind to explore precipitation estimation errors using TC across the United States (US). A multiplicative (logarithmic) error model is incorporated in the original TC formulation to relate the precipitation estimates to the unknown truth. For precipitation application, this is more realistic than the additive error model used in the original TC derivations, which is generally appropriate for existing applications such as in the case of wind vector components and soil moisture comparisons. This study provides error estimates of the precipitation products that can be incorporated into hydrological and meteorological models, especially those used in data assimilation. Physical interpretations of the error fields (related to topography, climate, etc) are explored. The methodology presented in this study could be used to quantify the uncertainties associated with precipitation estimates from each of the constellation of GPM satellites. Such quantification is prerequisite to optimally merging these estimates.

1 Introduction

Precipitation is one of the main drivers of the water cycle; therefore, accurate precipitation estimates are necessary for studying land–atmosphere interactions as well as linkages between the water, energy and carbon cycles. Surface precipitation is also a principal driver of hydrologic models with a wide range of applications. A wide suite of instruments (in-situ and remote sensing) monitor precipitation incident at the Earth surface. Specifically, there has been a great effort during the last two decades to use microwave radar and radiometer instruments on board low-earth orbit satellites to accurately estimate precipitation over large areas. These estimates when combined with infrared based cloud top temperature observations from geostationary satellites provide high spatial and temporal resolution precipitation estimates that are appropriate for hydrological and climatological studies.

However, precipitation estimation is inevitably subject to error. The errors are caused by different factors depending on the measurement instrument. For gauge measurements, the sparse distribution of gauges, environmental conditions such as wind and evaporation, and topography contribute to the errors. For ground-based radars, beam blockages in mountainous regions, the empirical backscatter-rain rate relationship (and the simplifications embededded in their functional form) and clutter are among the sources of error. Lastly, for satellite retrievals (both radiometer and radar), assumptions about the surface emissivity, neglecting evaporation below clouds, and empirical relationships are the driving factors of error.

The new Global Precipitation Measurement (GPM) mission aims to integrate precipitation estimates from a constellation of satellites to provide high spatial and temporal resolution estimates of precipitation over the Earth (Hou et al., 2013). However, successful data integration requires that the errors in each estimate are known. Since the truth is not known, only indirect methods are generally developed to estimate errors.

Several studies investigate and model the uncertainties in remotely-sensed precipitation estimates; however, they all depend on assuming the ground-based (gauge and/or radar) observations or models representing the zero-error precipitation (Krajewski et al., 2000; McCollum et al., 2002; Ebert et al., 2007; Su et al., 2008; Sapiano and Arkin, 2009; Tian et al., 2009; Vila et al., 2009; Anagnostou et al., 2010; Stampoulis and Anagnostou, 2012; Habib et al., 2012; Kirstetter et al., 2012; Chen et al., 2013; Kirstetter et al., 2013; Alemohammad et al., 2014; Maggioni et al., 2014; Seyyedi, 2014; Tang et al., 2014; Salio et al., 2014; Prat and Nelson, 2014; Gebregiorgis and Hossain, 2015; among others).

Triple Collocation (TC) provides a platform for quantifying the Root-Mean-Square-Error (RMSE) in three or more products that estimate the same geophysical variable. Developed by Stoffelen (1998), TC takes advantage of at least three spatially and temporally collocated measurements of the variable of interest to solve a system of equations and estimate the error variances of each of the measurements. To make this system of equations determined, some assumptions are built into the technique including zero error cross covariance between different products and zero covariance between errors and truth.

While TC has been used extensively to estimate errors in soil moisture products (Miralles et al., 2010; Dorigo et al., 2010; Parinussa et al., 2011; Anderson et al., 2012; Draper et al., 2013), it has also been successfully applied to other geophysical variables such as ocean wind speed and wave height (Stoffelen, 1998; Janssen et al., 2007; Portabella and Stoffelen, 2009), leaf area index (LAI) (Fang et al., 2012), fraction of absorbed photosynthetically active radiation (FAPAR) (D'Odorico et al., 2014), sea-ice thickness (Scott et al., 2014), atmospheric columnar integrated water vapor (Cimini et al., 2012; Thao et al., 2014), sea surface salinity (Ratheesh et al., 2013), and land water storage (van Dijk et al., 2014).

Roebeling et al. (2012) for the first time apply the TC technique to precipitation products and estimate errors for three precipitation products across Europe. The results show that a gridded gauge product and satellite retrievals (microwave) have TC errors less than 1.0 $\text{mm}\,\text{day}^{-1}$ while the European weather radar estimates have errors up to 18 $\text{mm}\,\text{day}^{-1}$ in some mountainous regions.

New variants of TC are introduced with wider applications in recent years. McColl et al. (2014) introduce the Extended TC (ETC) that can be used to easily estimate the correlation coefficient between each of the triplets and the unknown truth as well as their RMSEs. ETC is mathematically equivalent to the original TC; however, the ease

HESSD
12, 2527–2559, 2015

of calculating the correlation coefficients in ETC provides a different perspective on the performance of each product.

Su et al. (2014) introduce an implementation of instrument variables to reduce the minimum number of products necessary for TC analysis to two. In this framework, the lagged version of one of the two products is used as the third product to conduct the TC analysis (lagged-TC). If the lagged product is sampled at time intervals shorter than the temporal correlation length of the variable of interest, this approach can provide RMSE estimates of two collocated products.

In this study, we estimate the spatial RMSE between triplets of precipitation products across a central part of the US. Unlike Roebeling et al. (2012), we introduce a new logarithmic (multiplicative) error model that is more realistic for precipitation estimates. Moreover, the ETC approach is used in this study to estimate the correlation coefficients for each of the products.

Yilmaz and Crow (2014) present an extensive evaluation of the TC assumptions when applied to soil moisture products. We take a similar approach here, and use rain gauge data to validate the error estimates from TC analysis in a subset of pixels of the study domain. These pixels (located in the state of Oklahoma) have a dense network of rain gauges with a high quality data processing system that enables us to do this evaluation. The results of this evaluation provide a better understanding of the errors in precipitation products estimated by TC.

This paper is organized as following: Sect. 2 introduces the multiplicative TC analysis. Section 3 reviews the products used in this study. Section 4 presents the results of TC error estimates. Section 5 evaluates the assumptions of TC analysis using gauge data and Sect. 6 discusses the results and conclusions.

2 Triple Collocation formulation

In this section, we review the TC formulation and introduce the multiplicative error model. In the multiplicative error model for precipitation, the true precipitation is related

HESSD
12, 2527–2559, 2015

to the estimation as:

$$\boldsymbol{R}_i = a_i \boldsymbol{T}^{\beta_i} e^{\boldsymbol{\epsilon}_i} \tag{1}$$

in which $\boldsymbol{R}_i$ is the precipitation intensity estimate from product i, $\boldsymbol{T}$ is the true precipitation intensity, a_i is the multiplicative error, β_i is the deformation error and $\boldsymbol{\epsilon}_i$ is the residual (random) error. Variables that are in bold format indicate random variables. The multiplicative error model is used in several studies to investigate the errors associated with precipitation estimates (Hossain and Anagnostou, 2006; Ciach et al., 2007; Villarini et al., 2009; Tian et al., 2013). It is generally concluded that the multiplicative model is more appropriate for quantifying errors in precipitation estimates. Moreover, Tian et al. (2013) present a comparison between the linear and multiplicative error models applied to daily precipitation estimates across the US. They show that the multiplicative model has a better prediction skill and it is applicable to the variable and wide range of daily precipitation values.

In this study, we use the multiplicative model to relate the precipitation estimates to the true value; however, without having the truth or making any assumptions about the distribution of the error, we estimate the RMSE of each estimate. Taking the logarithm of Eq. (1), results in:

$$\ln(\boldsymbol{R}_i) = \alpha_i + \beta_i \ln(\boldsymbol{T}) + \boldsymbol{\epsilon}_i, \tag{2}$$

in which, $\alpha_i = \ln(a_i)$ is the offset. Defining $\boldsymbol{r}_i = \ln(\boldsymbol{R}_i)$ and $\boldsymbol{t} = \ln(\boldsymbol{T})$ the equation is simplified to:

$$\boldsymbol{r}_i = \alpha_i + \beta_i \boldsymbol{t} + \boldsymbol{\epsilon}_i. \tag{3}$$

This linear equation makes it possible to apply TC to the precipitation data assuming a multiplicative error model. Therefore, log-transformation of the precipitation estimates from all the products is performed in this study and then TC is applied. Assuming there are three collocated estimates of precipitation with zero mean residual errors

($E(\boldsymbol{\epsilon}_i) = 0$) that are uncorrelated with each other ($\mathrm{Cov}(\boldsymbol{\epsilon}_i, \boldsymbol{\epsilon}_j) = 0$) and with the true precipitation ($\mathrm{Cov}(\boldsymbol{\epsilon}_i, \boldsymbol{t}) = 0$), the RMSE of each product can be estimated using the following sets of equations (McColl et al., 2014):

$$\sigma^2_{\boldsymbol{r}_1} = C_{11} - \frac{C_{12}C_{13}}{C_{23},} \quad (4)$$

$$\sigma^2_{\boldsymbol{r}_2} = C_{22} - \frac{C_{12}C_{23}}{C_{13}}, \quad (5)$$

$$\sigma^2_{\boldsymbol{r}_3} = C_{33} - \frac{C_{13}C_{23}}{C_{12}}, \quad (6)$$

where C_{ij} is the (i,j)th element of the sample covariance matrix between the transformed triplets, and $\sigma_{\boldsymbol{r}_i}$ is the RMSE of the $\boldsymbol{r}_i$ product. Equations (4)–(6) estimate the mean-square-error of each product in logarithmic scale. In Sect. 4, the results of these estimates along with RMSE estimates of $\boldsymbol{R}_i$ products are presented.

Based on the ETC introduced by McColl et al. (2014), the correlation coefficient between the truth and each of the triplets is:

$$\rho^2_{\boldsymbol{t},1} = \frac{C_{12}C_{13}}{C_{11}C_{23}}, \quad (7)$$

$$\rho^2_{\boldsymbol{t},2} = \frac{C_{12}C_{23}}{C_{22}C_{13}}, \quad (8)$$

$$\rho^2_{\boldsymbol{t},3} = \frac{C_{13}C_{23}}{C_{33}C_{12}}, \quad (9)$$

where $\rho^2_{\boldsymbol{t},i}$ is the correlation coefficient between the truth and product i in the logarithmic scale (i.e. between $\boldsymbol{t}$ and $\boldsymbol{r}_i$). In defining the sign of the $\rho_{\boldsymbol{t},i}$, it is assumed that the measurements are positively correlated with the truth to overcome sign ambiguity.

HESSD
12, 2527–2559, 2015

Characterizing precipitation product errors across the US

S. H. Alemohammad et al.

3 Study domain and data pre-processing

Figure 1 shows the analysis domain and the spatial grid used in this study. The study domain ranges from 30 to 40° N latitudes and 110 to 80° W longitudes. This region is selected to maximize the overlapping spatial coverage between the data sets that are used here. Major water-bodies (Great Lakes and the Gulf of Mexico) and strong terrain (i.e. Rocky Mountains) are excluded.

Precipitation estimates from four products NEXRAD-IV, TRMM 3B42, GPI and GPCP are evaluated. NEXRAD-IV is the national mosaicked precipitation estimates from the National Weather Service ground-based WSR-88D radar network (Fulton et al., 1998). This product is based on merged gauge and radar estimates from 12 river forecast centers across the Continental United States (CONUS) that are mosaicked to a 4 km grid over CONUS. The product is available through the National Center for Atmospheric Research (NCAR) Earth Observing Laboratory (EOL; Lin and Mitchell, 2005). Using nearest neighbor sampling, we map this product to a $0.05^\circ \times 0.05^\circ$ latitude-longitude grid. The original NEXRAD-IV (hereafter called NEXRAD) product is hourly accumulation in mm and is available from January 2002 to present.

TRMM 3B42 is a multi-satellite precipitation estimate from the Tropical Rainfall Measuring Mission (TRMM) together with other low Earth-orbit microwave instruments (Huffman et al., 2007). The precipitation estimates from several microwave instruments are calibrated against the merged radar and radiometer precipitation product from TRMM, and then merged to produce a near-global 3 h precipitation product. The pixels with no microwave instrument observations are filled with measurements from IR instruments on board geostationary satellites. The TRMM 3B42 (hereafter called TRMM) is a gauge corrected product meaning that the monthly accumulation of estimates in each pixel are calibrated against GPCC gauge product to have similar monthly magnitudes. This product is available on a $0.25^\circ \times 0.25^\circ$ latitude-longitude grid from January 1998 to present. We use the current V7 of this product.

HESSD
12, 2527–2559, 2015

The GOES Precipitation Index (GPI) is a rainfall retrieval algorithm that only uses cloud-top temperatures from IR-based observations of geostationary satellites to estimate rain rate (Arkin and Meisner, 1987; Joyce and Arkin, 1997). The main advantage of this product is that it only uses observations from geostationary satellites that are frequently available across the globe. However, the physics of the precipitation process is not considered in this retrieval algorithm. Therefore, the estimates are only useful in the tropics and warm-season extra-tropics in which most of the precipitation originates from deep convective cloud systems. This product contains daily precipitation rates on a $1^\circ \times 1^\circ$ spatial grid from October 1996 to present.

The Global Precipitation Climatology Project (GPCP) is globally merged daily precipitation rate at $1^\circ \times 1^\circ$ spatial resolution from October 1996 to the present (Huffman et al., 2001). This is a merged estimate of precipitation from low earth orbit Passive Microwave (PMW) instruments, the GOES IR-based observations, and surface rain gauge measurements. The merging approach utilizes the higher accuracy of the PMW observations to calibrate the more frequent GOES observations. In this study, V1.2 of the One-Degree Daily (1DD) product of GPCP is used.

The NEXRAD and TRMM data are upscaled to a $1^\circ \times 1^\circ$ spatial grid to be consistent with the spatial resolution of the GPI and GPCP data.

The time domain for this error estimation study is from January 2002 until April 2014. All the data products have complete record within this time window which is more than one decade. Moreover, to generate temporally uncorrelated samples that do not have zero precipitation, the data from each product is temporally aggregated to biweekly values. A large number of zero values would violate the assumption that all errors are independent and identically distributed. Among the aggregated data, there are a few percentage of samples that have zero biweekly precipitation accumulation which are removed from the analysis. The percentage of samples with zero value is less than 2 % in most of the region other than 8 pixels in the southwest of the region (the driest part of the domain) that have up to 8 % of the samples equal to zero. In the accumulation

HESSD
12, 2527–2559, 2015

algorithm, any biweekly data with missing hourly or daily measurements is treated as a missing value.

This data aggregation reduces the number of samples across the temporal domain of this study. TC analysis needs enough samples to be able to provide an accurate estimation of the error. Therefore, we combine the estimates from four neighboring $1^\circ \times 1^\circ$ pixels to form data points for the $2^\circ \times 2^\circ$ grids shown in Fig. 1. This means measurements taken over each of the four $1^\circ \times 1^\circ$ pixels inside the $2^\circ \times 2^\circ$ pixel are each treated to be measurements over the $2^\circ \times 2^\circ$ pixel, increasing the total number of samples for each $2^\circ \times 2^\circ$ pixel. Under the assumption that the estimated rainfall is homogeneous over each $2^\circ \times 2^\circ$ pixel, we can trade off space and time in this way to increase the number of samples.

Figure 2 shows the climatology of precipitation derived from each of the four products. There is a good agreement between NEXRAD, TRMM and GPCP estimates; however, GPI has a different climatological pattern across the domain. This difference is not unexpected. GPI's retrieval algorithm is very simple and only considers the cloud top temperature; therefore, it is less accurate compared to the other three products that are either based on ground-based radar or have microwave estimates of precipitation combined with IR-based observations.

4 Results of TC analysis

In this section, we apply the multiplicative TC technique to the precipitation products introduced in Sect. 3 and present the estimated RMSE and correlation coefficients for each of the products. The four products are grouped to two triplets; Group 1 includes NEXRAD, TRMM and GPI products, and Group 2 includes NEXRAD, TRMM and GPCP. Similar results were obtained from other triplet combinations (not shown here).

Figures 3 and 4 show the RMSE of each $\boldsymbol{r}_i$ product in groups 1 and 2 respectively. These figures also show the number of data points (biweekly precipitation measurements) that are used in each pixel to do the TC estimate. Generally there are more than 1000 data points in each pixel. The sharp decline in the number of data points in the pixels in the south west of the study domain is due to the NEXRAD product, which had one of its radar systems repeatedly inactive during 2002 and 2003.

The RMSE reported in these figures is based on a bootstrap analysis. We run 1000 bootstrap simulations (i.e. sampling with replacement from the original data time series) and estimate the RMSE using Eqs. (4)–(6). The mean of these 1000 RMSE estimates are reported in Figs. 3 and 4. Additionally, the standard deviation (SD) of these bootstrap estimates is reported in the Supplement Fig. S1. The SDs of RMSE from the bootstrap simulations are one order of magnitude smaller than the RMSE estimate itself and the results are consistent between the two groups. GPI has a more uniform pattern for SD of RMSE compared to NEXRAD, TRMM and GPCP that have the east-west pattern. The SD plots provide a range of confidence on the RMSE estimates from TC analysis. Since the SDs are an order of magnitude smaller than the RMSE itself, the mean RMSE from the bootstrap simulations is a reasonable estimate of the RMSE.

The first observation and control check from Figs. 3 and 4 is that the RMSE estimates of precipitation from NEXRAD and TRMM in both of the groups are very similar. This shows that the TC analysis is robust and the results are not in general dependent on the choice of triplets. Moreover, TRMM product has a lower RMSE in most of the region.

The RMSE estimates shown in Figs. 3 and 4 are in logarithmic scale which are informative and useful if someone is assimilating the products in the logarithmic scale (equivalently using the $\boldsymbol{r}_i$ products). However, the RMSE estimates of $\boldsymbol{R}_i$ products in units of precipitation intensity (mm day^{-1} in this case) provide another perspective and might be simpler to interpret. Denoting $\mu_{\boldsymbol{R}_i}$ as the mean of $\boldsymbol{R}_i$, expansion of Eq. (2) using Taylor series results in:

$$\ln(\boldsymbol{R}_i) \approx \ln(\mu_{\boldsymbol{R}_i}) + (\boldsymbol{R}_i - \mu_{\boldsymbol{R}_i})\frac{1}{\mu_{\boldsymbol{R}_i}}. \quad (10)$$

Therefore,

$$\mathrm{Var}[\boldsymbol{r}_i] = \left(\frac{1}{\mu_{\boldsymbol{R}_i}}\right)^2 \mathrm{Var}[(\boldsymbol{R}_i - \mu_{\boldsymbol{R}_i})], \tag{11}$$

$$\sigma^2_{\boldsymbol{r}_i} = \left(\frac{1}{\mu_{\boldsymbol{R}_i}}\right)^2 \sigma^2_{\boldsymbol{R}_i}, \tag{12}$$

$$\sigma_{\boldsymbol{R}_i} = \mu_{\boldsymbol{R}_i}\sigma_{\boldsymbol{r}_i}. \tag{13}$$

Equation (13) is used to report the RMSE of each of the precipitation product errors after carrying out the TC analysis on the log-transformed products. Figures 5 and 6 show the RMSE of precipitation products in each group in units of mm day^{-1}. The SD of these RMSE estimate are also presented in Fig. S2 of Supplement.

There is again consistency between the results of NEXRAD and TRMM in both groups. Similar to Figs. 3 and 4, the RMSE of the TRMM product in both of the triplets is small compared to the other two products and is also relatively small compared to the mean precipitation from climatology maps in Fig. 2. NEXRAD has higher RMSE compared to TRMM, but is considerably smaller than GPCP or GPI.

Comparing the pattern of RMSE in NEXRAD, TRMM and GPCP with the climatology maps (Fig. 2), it is clear that the RMSE in each product increases east to west similar to the climatology. This means that in regions with higher mean precipitation rate, the RMSE is higher. This is consistent with other studies that have found that the mean error of precipitation estimates is proportional to the mean precipitation (Tian et al., 2013; Gebregiorgis and Hossain, 2014; Tang et al., 2014; Alemohammad et al., 2014, among others).

A recent study by Prat and Nelson (2014) investigates the error of several precipitation products (ground-based radar and microwave instruments) over CONUS by assuming the gauge data as truth. They mainly characterize the bias in precipitation estimates and evaluate detection of precipitation events at different intensity thresholds

HESSD
12, 2527–2559, 2015

and time scales. However, their results show a similar pattern in the error estimates; higher estimation errors for higher mean precipitation.

Figure 7 shows the estimated correlation coefficients between the underlying truth and each precipitation product in the logarithmic scale. Similar to Figs. S1 and S2 each column is showing the results of one of the triplet groups. Estimates of ρ^2 for TRMM and NEXRAD products from the two groups are very similar and again shows the robustness of results from the TC technique. Among the products analyzed here, the TRMM product has the highest correlation coefficient with the truth in almost all of the pixels. NEXRAD also has high correlation with the truth but there is a pattern that pixels toward the east of the region have higher correlation coefficients in the NEXRAD product. GPCP has less correlation with the truth, and it has a similar east-west pattern. GPI exhibits very low correlation coefficients (~ 0.1) toward the west of the region.

The combined and quantitative analyses of the RMSE estimate and the correlation coefficients show that the TRMM product has the best performance among the four products considered here. The RMSE and correlation coefficient for TRMM have little variations across the domain. This means that the TRMM product has better performance in diverse climatic and geographical conditions. The NEXRAD product has a distinct error pattern. Both the RMSE and correlation coefficient of the NEXRAD estimates are small toward the west of the domain. However, comparing the error estimates from NEXRAD with the climatology values reveals that the errors are sometimes on the same order as the climatology toward the west of the domain. This is also revealed by the correlation coefficient values, which have a smaller value in the west side of the domain for NEXRAD. This pattern is consistent with the NEXRAD coverage maps provided by Maddox et al. (2002) that shows the effect of terrain on radar beam blockage in mountainous regions of CONUS. Beam blockage is one of the sources of error in ground-based radar estimates of precipitation in mountainous regions.

The GPI and GPCP products have, in general, lower quality than TRMM and NEXRAD. They have higher RMSE and lower correlation coefficients with the truth. They both have the east-west pattern in the correlation coefficient; however, the GPI

HESSD
12, 2527–2559, 2015

product has a sharper gradient and is poorly correlated with the truth toward the west of the study domain. Precipitation events in this region are mostly driven by frontal systems; therefore, the GPI estimates that are solely based on cloud-top temperature are not well correlated with the truth. GPCP also uses IR-based observations of the clouds, but those are merged with microwave observations from low earth orbit satellites that are more accurate. Therefore, the resulting correlation coefficients are generally higher, especially in the west side of the study domain. If the analysis was limited to the RMSE estimates, GPI might be considered to be performing uniformly well across the entire domain. But with the correlation coefficients we can clearly see the change in quality of GPI estimates across the domain.

5 Gauge analysis

In this section we will review the assumptions that are embedded in TC estimates of RMSE and evaluate them using in-situ gauge data. Gauge data are used as a proxy for truth. As mentioned in Sect. 2, TC assumes zero correlation between errors of the triplets (zero error cross-covariance assumption) and between the errors and the truth (error orthogonality assumption). However, this assumption can be violated in many applications if the retrieval algorithms have similar error structures. Yilmaz and Crow (2014) investigated the assumptions of TC and introduced a decomposition of RMSE derived from TC as following:

$$\sigma^2_{\mathrm{TC}_1} = \sigma^2_{\mathrm{TRE}_1} + \sigma^2_{\mathrm{LS}_1} + \sigma^2_{\mathrm{OE}_1} + \sigma^2_{\mathrm{XCE}_1}. \quad (14)$$

In this equation, $\sigma^2_{\mathrm{TC}_1}$ is the error variance of product 1 that is estimated by TC, and $\sigma^2_{\mathrm{TRE}_1}$ is the true error variance of product 1 that TC is aiming to estimate. $\sigma^2_{\mathrm{LS}_1}$ is the leaked portion of σ^2_{T} (the variance of the true data), $\sigma^2_{\mathrm{OE}_1}$ represents the bias term due to the violation of error orthogonality assumption and $\sigma^2_{\mathrm{XCE}_1}$ is the bias term due

HESSD
12, 2527–2559, 2015

to the violation of zero error cross-covariance assumption between different products. Note, $\sigma^2_{\mathrm{XCE}_1}$ is affected by non-zero error cross covariance between any pair of the products, and it is not only between product 1 and the gauge. Using similar notations as in Sect. 2, these four elements are defined as:

$$\sigma^2_{\mathrm{TRE}_1} = \overline{\boldsymbol{\epsilon}_1 \boldsymbol{\epsilon}_1}, \tag{15}$$

$$\sigma^2_{\mathrm{LS}_1} = (\beta_1 - c_{3|1}\beta_3)(\beta_1 - c_{2|1}\beta_2)\sigma^2_{\boldsymbol{t}}, \tag{16}$$

$$\sigma^2_{\mathrm{OE}_1} = (\beta_1 - c_{3|1}\beta_3)(\overline{\boldsymbol{t}\boldsymbol{\epsilon}_1} - c_{2|1}\overline{\boldsymbol{t}\boldsymbol{\epsilon}_2}) + (\beta_1 - c_{2|1}\beta_2)(\overline{\boldsymbol{t}\boldsymbol{\epsilon}_1} - c_{3|1}\overline{\boldsymbol{t}\boldsymbol{\epsilon}_3}), \tag{17}$$

$$\sigma^2_{\mathrm{XCE}_1} = -c_{2|1}\overline{\boldsymbol{\epsilon}_1\boldsymbol{\epsilon}_2} - c_{3|1}\overline{\boldsymbol{\epsilon}_1\boldsymbol{\epsilon}_3} + c_{3|1}c_{2|1}\overline{\boldsymbol{\epsilon}_2\boldsymbol{\epsilon}_3}, \tag{18}$$

in which $c_{i|j}$ is the scaling factor of product i assuming product j as the reference and overbar refers to temporal averaging. Equations (15)–(18) indicate the error decomposition for product 1 in the triplet. Similar equations can be derived for other products. Derivations of equations for these decomposition terms using the multiplicative error model is presented in the Appendix.

For a detailed explanation on how to estimate different variables in these equations, the reader is referred to Sect. 2.c of Yilmaz and Crow (2014).

For this evaluation analysis we need accurate ground based observations in order to avoid errors due to differences in the spatial coverage between the gauges and the other products. The six pixels shown in Fig. 1 are selected for this evaluation since they have a dense network of rain gauges. These pixels are located in the state of Oklahoma and the gauge data are retrieved from the Oklahoma Mesonet network. This network provides quality controlled daily precipitation estimates across the state of Oklahoma from an automatic and spatially dense set of rain gauges. We have located the gauges in each of the pixels; each pixel at every time contains at least 12 gauges and some of the pixels have up to 39 monitoring gauges. The daily data from the gauges in each pixel are averaged to estimate the true rain of the pixel and are then accumulated to biweekly values.

HESSD
12, 2527–2559, 2015

S. H. Alemohammad et al.

It is understood that gauge data also have errors including representativeness error; however, as it is shown in Yilmaz and Crow (2014) (Appendix) the representativeness error causes a positive bias in the TC-based RMSE estimates while the cross correlation error causes a negative bias. Therefore, it is reasonable to assume gauge data as an unbiased estimate of truth. Moreover, in this study the average of estimates from several gauges is used as the unbiased estimate of the truth. The representativeness error of the gauge estimates is basically interpreted as part of the total error variance in the gauge product. However, since the gauge estimates are unbiased estimates of the truth, it can be used a proxy to decompose the error variance estimates from TC technique.

Figure 8 shows the results of error decomposition for the RMSE of the NEXRAD product. This figure shows that the bias caused by the leaked signal and error orthogonality assumption is almost zero in all of the cases. However, the zero error cross-covariance assumption is causing significant underestimation in the RMSE estimated by TC. Therefore, the NEXRAD RMSE estimate from TC is a lower bound for the error. Figures S3–S5 in the Supplement show similar decomposition of the RMSE in TRMM, GPCP and GPI products across these pixels. These figures also confirm that the violation of the zero cross covariance error leads to underestimation of the true RMSE by TC analysis. The noticeable difference between Figs. 8, S3, S4 and S5 is that in Fig. S5 that shows the error decomposition of GPI product the contribution of error cross covariance to the total TC estimate is small, and in four of the pixels is almost zero. This is consistent with the fact that GPI has a completely different retrieval algorithm and is only based on could top temperature measurements. Therefore, it has less correlation with other products. These results are consistent with the findings in Yilmaz and Crow (2014). Moreover, this analysis shows that similar to the soil moisture data it is appropriate to assume that the errors of precipitation products are not correlated with the truth.

The estimates in Fig. 8 are based on another bootstrap simulation with 1000 samples, with corresponding one SD confidence intervals.

HESSD
12, 2527–2559, 2015

6 Conclusions

This study presents, for the first time, error estimates of four precipitation products across a central part of the continental US using Triple Collocation (TC). A multiplicative error model is introduced to TC analysis that is a more realistic error model for precipitation. Furthermore, an extended version of TC is used with which not only the SD of random errors in each product, but the correlation coefficient of each product with respect to an underlying truth are estimated. The results show that the TRMM product is performing relatively better than the other three products. TRMM has the lowest RMSE across the domain, and the highest correlation coefficient with the underlying truth. Meanwhile, NEXRAD performs relatively poorly in the west side of the study domain that is probably caused by the terrain beam blockage. The performance of the GPCP and GPI product were lower than that of TRMM and NEXRAD. GPI has significantly lower performance in the west side of the study domain that is likely caused by the simple retrieval algorithm used in this product. Meanwhile, GPI has a reasonably good correlation with the underlying truth in the east side of the domain.

In the second part of the paper, an evaluation of the assumptions built into TC is carried out using surface gauge data as proxy for the truth across selective pixels. These pixels have a dense coverage of in-situ gauges. The results of this evaluation reveal that the TC error estimates underestimate the true error in different products due to a violation of the assumption of zero error cross covariance. However, the result of RMSE estimates from TC have a lot of potential to be incorporated into data assimilation and data merging algorithms.

Triple Collocation analysis has a lot of potential to be applied to various precipitation products at a wide range of spatial and temporal resolutions. This will provide a better understanding of the true error patterns in different products. Error quantification of precipitation products is a necessity if one aims to merge precipitation estimates from several instruments/models. However, care should be taken in choosing triplets

HESSD
12, 2527–2559, 2015

that have zero or small error cross covariance. Otherwise, the error variances will be underestimated.

The multiplicative error model used in this study is shown to be an appropriate choice relative to the additive model. However, it would be beneficial to investigate more complex models that can take into account any higher order dependence of the estimate on the truth. A modification to this study would be to include a gauge-only precipitation product. This would reduce the error cross covariance between the products, since the gauge measurement system is different from the remote-sensing instruments. Although gauge estimates have representativeness error, this error will be part of the total error in the gauge product resulting in higher RMSE values of gauge product. Furthermore, conducting TC analysis on precipitation data with different temporal resolution will provide valuable insight on the performance of different products at different temporal scales. However, this should be carried out with care, as precipitation errors at certain temporal resolutions are highly correlated and are not appropriate for TC analysis.

Appendix: Error decomposition

In this section, we derive Eqs. (15)–(18) starting with the multiplicative error model in logarithmic scale:

$$\boldsymbol{r}_i = \alpha_i + \beta_i \boldsymbol{t} + \boldsymbol{\epsilon}_i. \tag{A1}$$

Without loss of generality, we assume $\boldsymbol{r}_i$ and $\boldsymbol{t}$ be the anomalies from a climatological mean; then, the model is simplified to:

$$\boldsymbol{r}_i = \beta_i \boldsymbol{t} + \boldsymbol{\epsilon}_i. \tag{A2}$$

HESSD
12, 2527–2559, 2015

Characterizing precipitation product errors across the US

S. H. Alemohammad et al.

Choosing product $\boldsymbol{r}_1$ as the reference, the scaling factors are defined as:

$$c_{2|1} = \frac{\overline{\boldsymbol{r}_1\boldsymbol{r}_3}}{\overline{\boldsymbol{r}_2\boldsymbol{r}_3}}, \tag{A3}$$

$$c_{3|1} = \frac{\overline{\boldsymbol{r}_1\boldsymbol{r}_2}}{\overline{\boldsymbol{r}_3\boldsymbol{r}_2}}. \tag{A4}$$

Therefore, the rescaled data sets are defined as: $\boldsymbol{r}_2^* = c_{2|1}\boldsymbol{r}_2$ and $\boldsymbol{r}_3^* = c_{3|1}\boldsymbol{r}_3$. Then, TC-based error variance of product 1 is defined as:

$$\sigma^2_{\mathrm{TC}_1} = \overline{(\boldsymbol{r}_1 - \boldsymbol{r}_3^*)(\boldsymbol{r}_1 - \boldsymbol{r}_2^*)}. \tag{A5}$$

Inserting $\boldsymbol{r}_2^*$, $\boldsymbol{r}_3^*$ and Eq. (A2) into Eq. (A5):

$$\sigma^2_{\mathrm{TC}_1} = \overline{[(\beta_1 - c_{3|1}\beta_3)\boldsymbol{t} + (\boldsymbol{\epsilon}_1 - c_{3|1}\boldsymbol{\epsilon}_3)][(\beta_1 - c_{2|1}\beta_2)\boldsymbol{t} + (\boldsymbol{\epsilon}_1 - c_{2|1}\boldsymbol{\epsilon}_2)]}, \tag{A6}$$

$$\begin{aligned}\sigma^2_{\mathrm{TC}_1} &= (\beta_1 - c_{3|1}\beta_3)(\beta_1 - c_{2|1}\beta_2)\sigma^2_{\boldsymbol{t}} \\ &+ (\beta_1 - c_{3|1}\beta_3)(\overline{\boldsymbol{t}\boldsymbol{\epsilon}_1} - c_{2|1}\overline{\boldsymbol{t}\boldsymbol{\epsilon}_2}) + (\beta_1 - c_{2|1}\beta_2)(\overline{\boldsymbol{t}\boldsymbol{\epsilon}_1} - c_{3|1}\overline{\boldsymbol{t}\boldsymbol{\epsilon}_3}) \\ &+ (\overline{\boldsymbol{\epsilon}_1\boldsymbol{\epsilon}_1} - c_{2|1}\overline{\boldsymbol{\epsilon}_1\boldsymbol{\epsilon}_2} - c_{3|1}\overline{\boldsymbol{\epsilon}_1\boldsymbol{\epsilon}_3} + c_{3|1}c_{2|1}\overline{\boldsymbol{\epsilon}_2\boldsymbol{\epsilon}_3}).\end{aligned} \tag{A7}$$

Rewriting Eq. (A7) as:

$$\sigma^2_{\mathrm{TC}_1} = \sigma^2_{\mathrm{TRE}_1} + \sigma^2_{\mathrm{LS}_1} + \sigma^2_{\mathrm{OE}_1} + \sigma^2_{\mathrm{XCE}_1}, \tag{A8}$$

where:

$$\sigma^2_{\mathrm{TRE}_1} = \overline{\boldsymbol{\epsilon}_1\boldsymbol{\epsilon}_1}, \tag{A9}$$

$$\sigma^2_{\mathrm{LS}_1} = (\beta_1 - c_{3|1}\beta_3)(\beta_1 - c_{2|1}\beta_2)\sigma^2_{\boldsymbol{t}}, \tag{A10}$$

$$\sigma^2_{\mathrm{OE}_1} = (\beta_1 - c_{3|1}\beta_3)(\overline{\boldsymbol{t}\boldsymbol{\epsilon}_1} - c_{2|1}\overline{\boldsymbol{t}\boldsymbol{\epsilon}_2}) + (\beta_1 - c_{2|1}\beta_2)(\overline{\boldsymbol{t}\boldsymbol{\epsilon}_1} - c_{3|1}\overline{\boldsymbol{t}\boldsymbol{\epsilon}_3}), \tag{A11}$$

$$\sigma^2_{\mathrm{XCE}_1} = -c_{2|1}\overline{\boldsymbol{\epsilon}_1\boldsymbol{\epsilon}_2} - c_{3|1}\overline{\boldsymbol{\epsilon}_1\boldsymbol{\epsilon}_3} + c_{3|1}c_{2|1}\overline{\boldsymbol{\epsilon}_2\boldsymbol{\epsilon}_3}. \tag{A12}$$

HESSD
12, 2527–2559, 2015

Characterizing precipitation product errors across the US

S. H. Alemohammad et al.

Equations (A9)–(A12) are the same as Eqs. (15)–(18) that are used to decompose the RMSE estimates of TC analysis.

The Supplement related to this article is available online at doi:10.5194/hessd-12-2527-2015-supplement.

Acknowledgements. The authors wish to thank all the producers and distributors of the data used in this study. The TRMM data used in this study were acquired as part of the NASA's Earth-Sun System Division and archived and distributed by the Goddard Earth Sciences (GES) Data and Information Services Center (DISC). The GPCP 1DD data were provided by the NASA/Goddard Space Flight Center's Mesoscale Atmospheric Processes Laboratory, which develops and computes the 1DD as a contribution to the GEWEX Global Precipitation Climatology Project. The GPI data are produced by science investigators, Phillip Arkin and John Janowiak of the Climate Analysis Center, NOAA, Washington, D.C., and distributed by the Distributed Active Archive Center (Code 610.2) at the Goddard Space Flight Center, Greenbelt, MD, 20771. The Oklahoma Mesonet data are provided courtesy of the Oklahoma Mesonet, a cooperative venture between Oklahoma State University and The University of Oklahoma and supported by the taxpayers of Oklahoma.

References

Alemohammad, S. H., Entekhabi, D., and McLaughlin, D. B.: Evaluation of long-term SSM/I-based precipitation records over land, J. Hydrometeorol., 15, 2012–2029, doi:10.1175/JHM-D-13-0171.1, 2014. 2529, 2538

Anagnostou, E., Maggioni, V., Nikolopoulos, E., Meskele, T., Hossain, F., and Papadopoulos, A.: Benchmarking high-resolution global satellite rainfall products to radar and rain-gauge rainfall estimates, IEEE T. Geosci. Remote, 48, 1667–1683, doi:10.1109/TGRS.2009.2034736, 2010. 2529

Anderson, W. B., Zaitchik, B. F., Hain, C. R., Anderson, M. C., Yilmaz, M. T., Mecikalski, J., and Schultz, L.: Towards an integrated soil moisture drought monitor for East Africa, Hydrol. Earth Syst. Sci., 16, 2893–2913, doi:10.5194/hess-16-2893-2012, 2012. 2530

Arkin, P. A. and Meisner, B. N.: The relationship between large-scale convective rainfall and cold cloud over the Western Hemisphere during 1982–84, Mon. Weather Rev., 115, 51–74, doi:10.1175/1520-0493(1987)115<0051:TRBLSC>2.0.CO;2, 1987. 2535

Chen, S., Kirstetter, P. E., Hong, Y., Gourley, J. J., Tian, Y. D., Qi, Y. C., Cao, Q., Zhang, J., Howard, K., Hu, J. J., and Xue, X. W.: Evaluation of spatial errors of precipitation rates and types from TRMM spaceborne radar over the southern CONUS, J. Hydrometeorol., 14, 1884–1896, doi:10.1175/JHM-D-13-027.1, 2013. 2529

Ciach, G. J., Krajewski, W. F., and Villarini, G.: Product-error-driven uncertainty model for probabilistic quantitative precipitation estimation with NEXRAD data, J. Hydrometeorol., 8, 1325–1347, doi:10.1175/2007JHM814.1, 2007. 2532

Cimini, D., Pierdicca, N., Pichelli, E., Ferretti, R., Mattioli, V., Bonafoni, S., Montopoli, M., and Perissin, D.: On the accuracy of integrated water vapor observations and the potential for mitigating electromagnetic path delay error in InSAR, Atmos. Meas. Tech., 5, 1015–1030, doi:10.5194/amt-5-1015-2012, 2012. 2530

D'Odorico, P., Gonsamo, A., Pinty, B., Gobron, N., Coops, N., Mendez, E., and Schaepman, M. E.: Intercomparison of fraction of absorbed photosynthetically active radiation products derived from satellite data over Europe, Remote Sens. Environ., 142, 141–154, doi:10.1016/j.rse.2013.12.005, 2014. 2530

Dorigo, W. A., Scipal, K., Parinussa, R. M., Liu, Y. Y., Wagner, W., de Jeu, R. A. M., and Naeimi, V.: Error characterisation of global active and passive microwave soil moisture datasets, Hydrol. Earth Syst. Sci., 14, 2605–2616, doi:10.5194/hess-14-2605-2010, 2010. 2530

Draper, C., Reichle, R., de Jeu, R., Naeimi, V., Parinussa, R., and Wagner, W.: Estimating root mean square errors in remotely sensed soil moisture over continental scale domains, Remote Sens. Environ., 137, 288–298, doi:10.1016/j.rse.2013.06.013, 2013. 2530

Ebert, E. E., Janowiak, J. E., and Kidd, C.: Comparison of near-real-time precipitation estimates from satellite observations and numerical models, B. Am. Meteorol. Soc., 88, 47–64, doi:10.1175/BAMS-88-1-47, 2007. 2529

Fang, H., Wei, S., Jiang, C., and Scipal, K.: Theoretical uncertainty analysis of global MODIS, CYCLOPES, and {GLOBCARBON} {LAI} products using a triple collocation method, Remote Sens. Environ., 124, 610–621, doi:10.1016/j.rse.2012.06.013, 2012. 2530

HESSD
12, 2527–2559, 2015

Fulton, R. A., Breidenbach, J. P., Seo, D.-J., Miller, D. A., and O'Bannon, T.: The WSR-88D rainfall algorithm, Weather Forecast., 13, 377–395, doi:10.1175/1520-0434(1998)013<0377:TWRA>2.0.CO;2, 1998. 2534

Gebregiorgis, A. and Hossain, F.: Estimation of satellite rainfall error variance using readily available geophysical features, IEEE T. Geosci. Remote, 52, 288–304, doi:10.1109/TGRS.2013.2238636, 2014. 2538

Gebregiorgis, A. S. and Hossain, F.: How well can we estimate error variance of satellite precipitation data around the world?, Atmos. Res., 154, 39–59, doi:10.1016/j.atmosres.2014.11.005, 2015. 2530

Habib, E., Haile, A. T., Tian, Y., and Joyce, R. J.: Evaluation of the high-resolution CMORPH satellite rainfall product using dense rain gauge observations and radar-based estimates, J. Hydrometeorol., 13, 1784–1798, doi:10.1175/JHM-D-12-017.1, 2012. 2529

Hossain, F. and Anagnostou, E. N.: A two-dimensional satellite rainfall error model, IEEE T. Geosci. Remote, 44, 1511–1522, doi:10.1109/TGRS.2005.863866, 2006. 2532

Hou, A. Y., Kakar, R. K., Neeck, S., Azarbarzin, A. A., Kummerow, C. D., Kojima, M., Oki, R., Nakamura, K., and Iguchi, T.: The global precipitation measurement mission, B. Am. Meteorol. Soc., 95, 701–722, doi:10.1175/BAMS-D-13-00164.1, 2013. 2529

Huffman, G. J., Adler, R. F., Morrissey, M. M., Bolvin, D. T., Curtis, S., Joyce, R., McGavock, B., and Susskind, J.: Global precipitation at one-degree daily resolution from multisatellite observations, J. Hydrometeorol., 2, 36–50, doi:10.1175/1525-7541(2001)002<0036:GPAODD>2.0.CO;2, 2001. 2535

Huffman, G. J., Bolvin, D. T., Nelkin, E. J., Wolff, D. B., Adler, R. F., Gu, G., Hong, Y., Bowman, K. P., and Stocker, E. F.: The TRMM Multisatellite Precipitation Analysis (TMPA): quasi-global, multiyear, combined-sensor precipitation estimates at fine scales, J. Hydrometeorol., 8, 38–55, doi:10.1175/JHM560.1, 2007. 2534

Janssen, P. A. E. M., Abdalla, S., Hersbach, H., and Bidlot, J.-R.: Error estimation of Buoy, satellite, and model wave height data, J. Atmos. Ocean. Tech., 24, 1665–1677, doi:10.1175/JTECH2069.1, 2007. 2530

Joyce, R. and Arkin, P. A.: Improved estimates of tropical and subtropical precipitation using the GOES precipitation index, J. Atmos. Ocean. Tech., 14, 997–1011, doi:10.1175/1520-0426(1997)014<0997:IEOTAS>2.0.CO;2, 1997. 2535

Kirstetter, P.-E., Hong, Y., Gourley, J. J., Schwaller, M., Petersen, W., and Zhang, J.: Comparison of TRMM 2A25 products, version 6 and version 7, with NOAA/NSSL ground radar-based national mosaic QPE, J. Hydrometeorol., 14, 661–669, doi:10.1175/JHM-D-12-030.1, 2012. 2529

Kirstetter, P.-E., Viltard, N., and Gosset, M.: An error model for instantaneous satellite rainfall estimates: evaluation of BRAIN-TMI over West Africa, Q. J. Roy. Meteor. Soc., 139, 894–911, doi:10.1002/qj.1964, 2013. 2529

Krajewski, W. F., Ciach, G. J., McCollum, J. R., and Bacotiu, C.: Initial validation of the global precipitation climatology project monthly rainfall over the United States, J. Appl. Meteorol., 39, 1071–1086, doi:10.1175/1520-0450(2000)039<1071:IVOTGP>2.0.CO;2, 2000. 2529

Lin, Y. and Mitchell, K. E.: The NCEP Stage II/IV hourly precipitation analyses: development and applications, in: 19th Conf. on Hydrology, American Meteorological Society, San Diego, CA, January 2005, Paper 1.2, available at: http://www.emc.ncep.noaa.gov/mmb/ylin/pcpanl/refs/stage2-4.19hydro.pdf (last access: 29 December 2014), 2005. 2534

Maddox, R. A., Zhang, J., Gourley, J. J., and Howard, K. W.: Weather radar coverage over the contiguous United States, Weather Forecast., 17, 927–934, doi:10.1175/1520-0434(2002)017<0927:WRCOTC>2.0.CO;2, 2002. 2539

Maggioni, V., Sapiano, M. R. P., Adler, R. F., Tian, Y., and Huffman, G. J.: An error model for uncertainty quantification in high-time-resolution precipitation products, J. Hydrometeorol., 15, 1274–1292, doi:10.1175/JHM-D-13-0112.1, 2014. 2529

McColl, K. A., Vogelzang, J., Konings, A. G., Entekhabi, D., Piles, M., and Stoffelen, A.: Extended triple collocation: estimating errors and correlation coefficients with respect to an unknown target, Geophys. Res. Lett., 41, 6229–6236, doi:10.1002/2014GL061322, 2014. 2530, 2533

McCollum, J. R., Krajewski, W. F., Ferraro, R. R., and Ba, M. B.: Evaluation of biases of satellite rainfall estimation algorithms over the continental United States, J. Appl. Meteorol., 41, 1065–1080, doi:10.1175/1520-0450(2002)041<1065:EOBOSR>2.0.CO;2, 2002. 2529

Miralles, D. G., Crow, W. T., and Cosh, M. H.: Estimating spatial sampling errors in coarse-scale soil moisture estimates derived from point-scale observations, J. Hydrometeorol., 11, 1423–1429, doi:10.1175/2010JHM1285.1, 2010. 2530

Parinussa, R. M., Holmes, T. R. H., Yilmaz, M. T., and Crow, W. T.: The impact of land surface temperature on soil moisture anomaly detection from passive microwave observations, Hydrol. Earth Syst. Sci., 15, 3135–3151, doi:10.5194/hess-15-3135-2011, 2011. 2530

Portabella, M. and Stoffelen, A.: On scatterometer ocean stress, J. Atmos. Ocean. Tech., 26, 368–382, doi:10.1175/2008JTECHO578.1, 2009. 2530

Prat, O. P. and Nelson, B. R.: Evaluation of precipitation estimates over CONUS derived from satellite, radar, and rain gauge datasets (2002–2012), Hydrol. Earth Syst. Sci. Discuss., 11, 11489–11531, doi:10.5194/hessd-11-11489-2014, 2014. 2530, 2538

Ratheesh, S., Mankad, B., Basu, S., Kumar, R., and Sharma, R.: Assessment of satellite-derived sea surface salinity in the Indian Ocean, IEEE Geosci. Remote S., 10, 428–431, doi:10.1109/LGRS.2012.2207943, 2013. 2530

Roebeling, R. A., Wolters, E. L. A., Meirink, J. F., and Leijnse, H.: Triple collocation of summer precipitation retrievals from SEVIRI over Europe with gridded rain gauge and weather radar data, J. Hydrometeorol., 13, 1552–1566, doi:10.1175/JHM-D-11-089.1, 2012. 2530, 2531

Salio, P., Hobouchian, M. P., Skabar, Y. G., and Vila, D.: Evaluation of high-resolution satellite precipitation estimates over southern South America using a dense rain gauge network, Atmos. Res., doi:10.1016/j.atmosres.2014.11.017, online first, 2014. 2530

Sapiano, M. R. P. and Arkin, P. A.: An intercomparison and validation of high-resolution satellite precipitation estimates with 3-hourly gauge data, J. Hydrometeorol., 10, 149–166, doi:10.1175/2008JHM1052.1, 2009. 2529

Scott, K., Buehner, M., and Carrieres, T.: An assessment of sea-ice thickness along the Labrador coast from AMSR-E and MODIS data for operational data assimilation, IEEE T. Geosci. Remote, 52, 2726–2737, doi:10.1109/TGRS.2013.2265091, 2014. 2530

Seyyedi, H.: Performance Assessment of Satellite Rainfall Products for Hydrologic Modeling, Ph. D. thesis, University of Connecticut, Storrs, CT, USA, available at: http://digitalcommons.uconn.edu/dissertations/335, last access: 29 December, 2014. 2529

Stampoulis, D. and Anagnostou, E. N.: Evaluation of global satellite rainfall products over continental Europe, J. Hydrometeorol., 13, 588–603, doi:10.1175/JHM-D-11-086.1, 2012. 2529

Stoffelen, A.: Toward the true near-surface wind speed: error modeling and calibration using triple collocation, J. Geophys. Res.-Oceans, 103, 7755–7766, doi:10.1029/97JC03180, 1998. 2530

Su, C.-H., Ryu, D., Crow, W. T., and Western, A. W.: Beyond triple collocation: applications to soil moisture monitoring, J. Geophys. Res.-Atmos., 119, 6419–6439, doi:10.1002/2013JD021043, 2014. 2531

Su, F., Hong, Y., and Lettenmaier, D. P.: Evaluation of TRMM multisatellite precipitation analysis (TMPA) and its utility in hydrologic prediction in the La Plata Basin, J. Hydrometeorol., 9, 622–640, doi:10.1175/2007JHM944.1, 2008. 2529

Tang, L., Tian, Y., and Lin, X.: Validation of precipitation retrievals over land from satellite-based passive microwave sensors, J. Geophys. Res.-Atmos., 119, 4546–4567, doi:10.1002/2013JD020933, 2014. 2530, 2538

Thao, S., Eymard, L., Obligis, E., and Picard, B.: Trend and variability of the atmospheric water vapor: a mean sea level issue, J. Atmos. Ocean. Tech., 31, 1881–1901, doi:10.1175/JTECH-D-13-00157.1, 2014. 2530

Tian, Y., Peters-Lidard, C. D., Eylander, J. B., Joyce, R. J., Huffman, G. J., Adler, R. F., Hsu, K.-I., Turk, F. J., Garcia, M., and Zeng, J.: Component analysis of errors in satellite-based precipitation estimates, J. Geophys. Res.-Atmos., 114, D24101, doi:10.1029/2009JD011949, 2009. 2529

Tian, Y., Huffman, G. J., Adler, R. F., Tang, L., Sapiano, M., Maggioni, V., and Wu, H.: Modeling errors in daily precipitation measurements: additive or multiplicative?, Geophys. Res. Lett., 40, 2060–2065, doi:10.1002/grl.50320, 2013. 2532, 2538

van Dijk, A. I. J. M., Renzullo, L. J., Wada, Y., and Tregoning, P.: A global water cycle reanalysis (2003–2012) merging satellite gravimetry and altimetry observations with a hydrological multi-model ensemble, Hydrol. Earth Syst. Sci., 18, 2955–2973, doi:10.5194/hess-18-2955-2014, 2014. 2530

Vila, D. A., de Goncalves, L. G. G., Toll, D. L., and Rozante, J. R.: Statistical evaluation of combined daily gauge observations and rainfall satellite estimates over continental South America, J. Hydrometeorol., 10, 533–543, doi:10.1175/2008JHM1048.1, 2009. 2529

Villarini, G., Krajewski, W. F., Ciach, G. J., and Zimmerman, D. L.: Product-error-driven generator of probable rainfall conditioned on WSR-88D precipitation estimates, Water Resour. Res., 45, W01404, doi:10.1029/2008WR006946, 2009. 2532

Yilmaz, M. T. and Crow, W. T.: Evaluation of assumptions in soil moisture triple collocation analysis, J. Hydrometeorol., 15, 1293–1302, doi:10.1175/JHM-D-13-0158.1, 2014. 2531, 2540, 2541, 2542

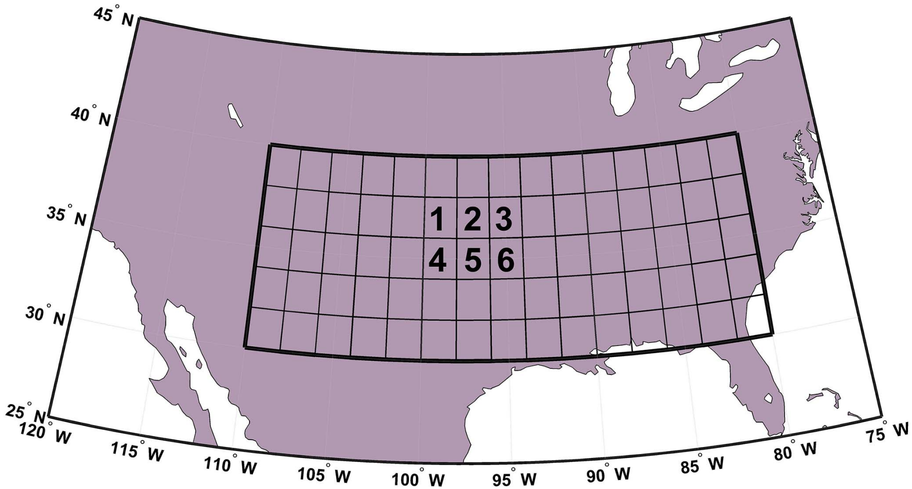

Figure 1. Study Domain. The six numbered pixels are used in Sect. 5 for evaluation of TC assumptions in estimating RMSE.

HESSD
12, 2527–2559, 2015

Characterizing precipitation product errors across the US

S. H. Alemohammad et al.

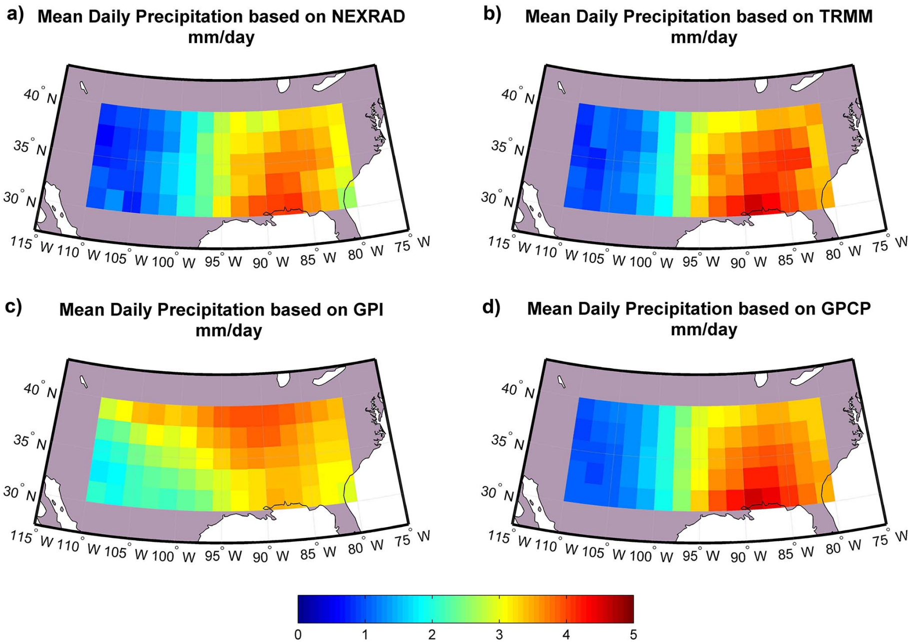

Figure 2. Climatology of precipitation across the study domain from each of the products.

HESSD
12, 2527–2559, 2015

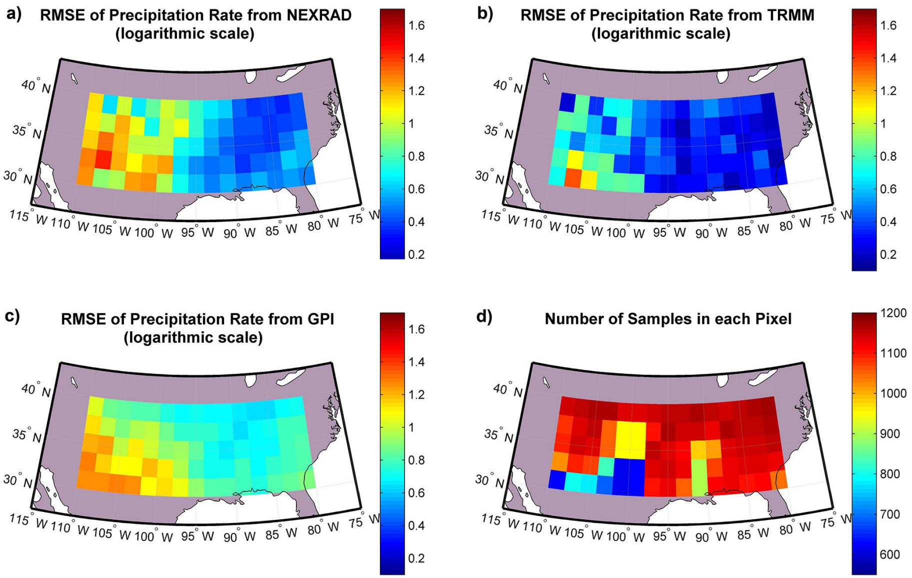

Figure 3. RMSE of the precipitation rate in logarithmic scale estimated from TC using triplets in group 1; **(a)** NEXRAD, **(b)** TRMM, **(c)** GPI. Panel **(d)** shows the number of data points (biweekly measurements) in each pixel that are used for error estimation in TC analysis.

HESSD
12, 2527–2559, 2015
Characterizing precipitation product errors across the US
S. H. Alemohammad et al.

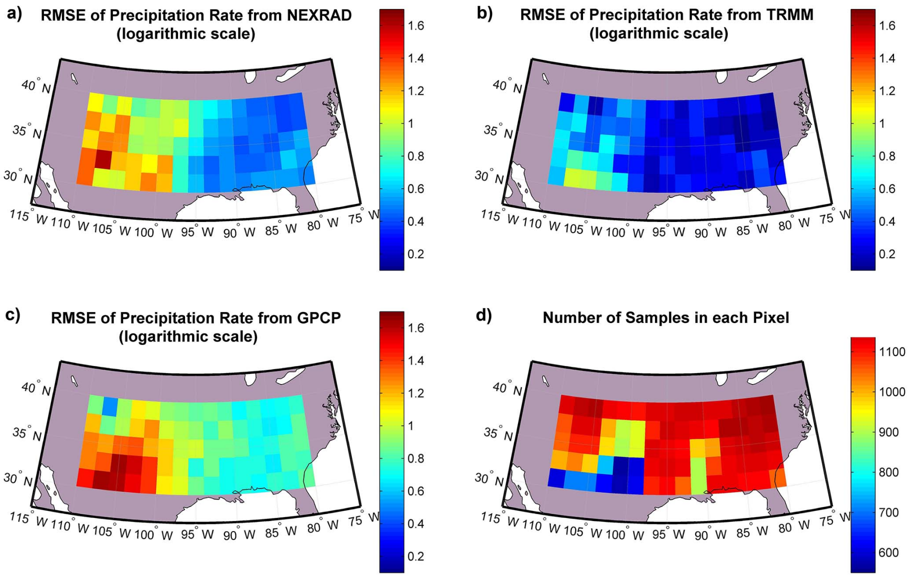

Figure 4. RMSE of the precipitation rate in logarithmic scale estimated from TC using triplets in group 2; **(a)** NEXRAD, **(b)** TRMM, **(c)** GPI. Panel **(d)** shows the number of data points (biweekly measurements) in each pixel that are used for error estimation in TC analysis.

HESSD
12, 2527–2559, 2015

S. H. Alemohammad et al.

Title Page
Abstract | Introduction
Conclusions | References
Tables | Figures
◀| |▶
◀ ▶
Back | Close
Full Screen / Esc
Printer-friendly Version
Interactive Discussion

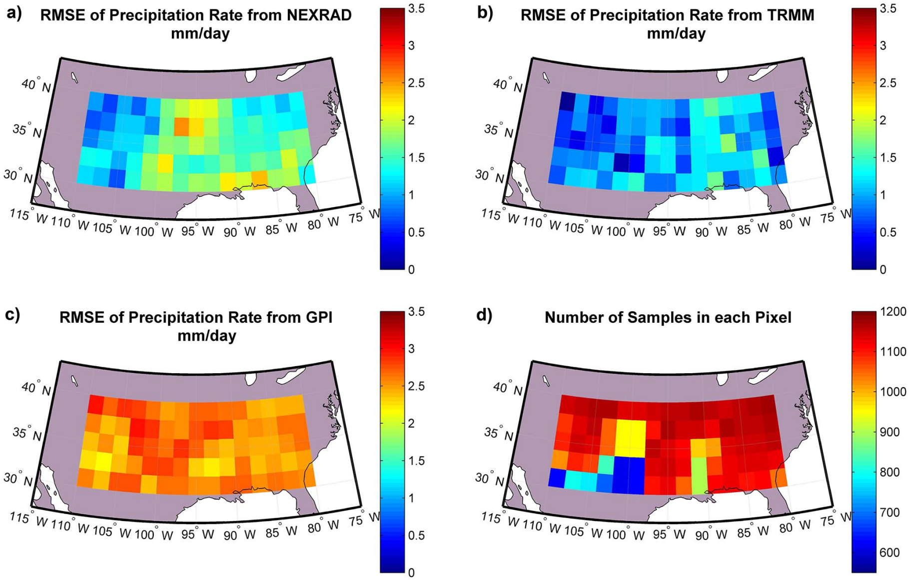

Figure 5. RMSE of the precipitation rate estimated from TC using triplets in group 1; **(a)** NEXRAD, **(b)** TRMM, **(c)** GPI. Panel **(d)** shows the number of data points (biweekly measurements) in each pixel that are used for error estimation in TC analysis.

HESSD
12, 2527–2559, 2015

Title Page
Abstract | Introduction
Conclusions | References
Tables | Figures
◀| |▶
◀ ▶
Back | Close
Full Screen / Esc
Printer-friendly Version
Interactive Discussion

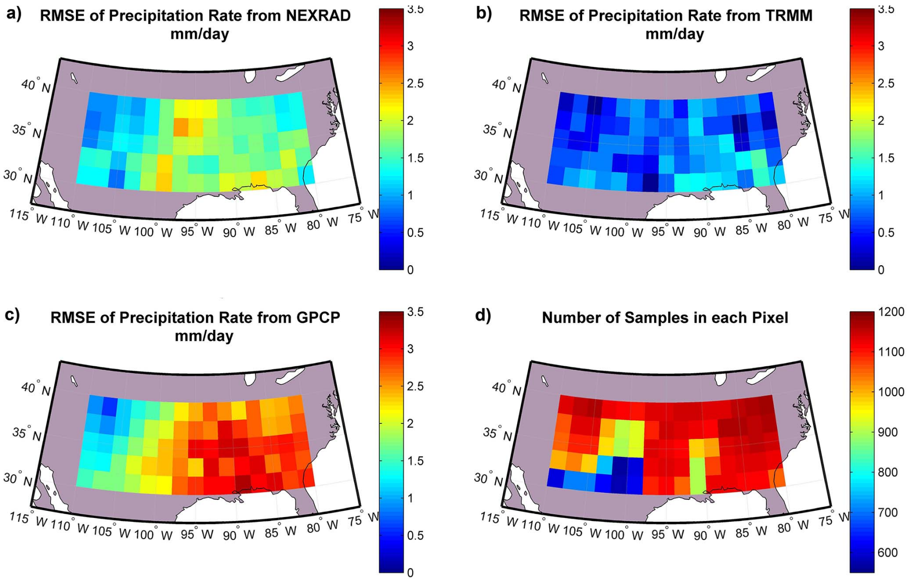

Figure 6. RMSE of the precipitation rate estimated from TC using triplets in group 2; **(a)** NEXRAD, **(b)** TRMM, **(c)** GPCP. Panel **(d)** shows the number of datapoints (biweekly measurements) in each pixel that are used for error estimation in TC analysis.

HESSD
12, 2527–2559, 2015

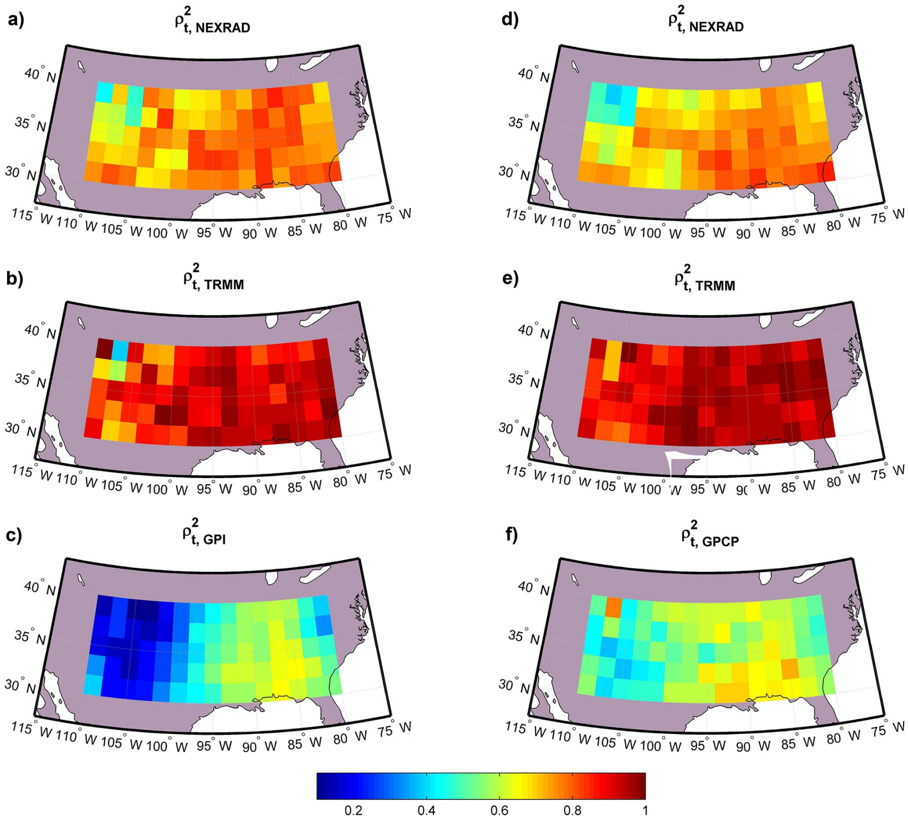

Figure 7. Correlation coefficient between the truth and each precipitation product. The left column shows the results for triplets in group 1, and the right column shows the results for triplets in group 2.

HESSD
12, 2527–2559, 2015

S. H. Alemohammad et al.

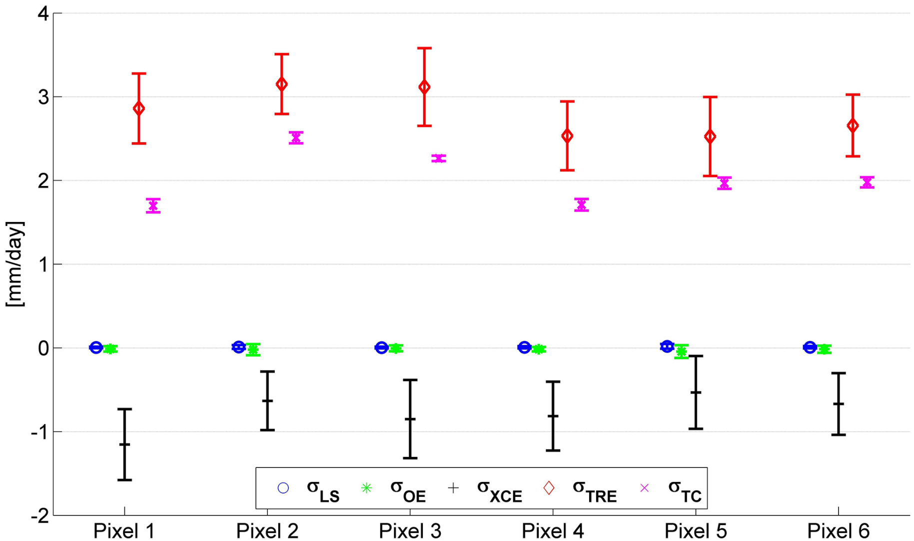

Figure 8. Decomposition of TC-based estimate of RMSE in the NEXRAD product across the six pixels shown in Fig. 1. Error bars show one SD of the estimates from a bootstrap run with 100 samples.

HESSD
12, 2527–2559, 2015

Characterizing precipitation product errors across the US

S. H. Alemohammad et al.